RESEARCH ARTICLE

Development, Optimization and Characterization of Glimepiride Nanosuspension with Improved Solubility and Dissolution

Padmnabh*, DC Bhatt

Department of Pharmaceutical Sciences, Guru Jambheshwar University of Science and Technology, Hisar, Haryana, India.

Received: 27th September, 2023; Revised: 29th October, 2023; Accepted: 10th November, 2023; Available Online: 25th December, 2023

ABSTRACT

Current work describes the development of nanoparticulate suspension (NPs) of glimeperide (GLMP) with enhanced solubility and bioavailability. Using the ultrasonication-assisted precipitation method, GLMP-NP was developed and optimized through the use of a three-factor two-level full factorial design methodology. Drug release, size of a particle, and encapsulation efficiency from nanoparticles were considered as dependent variables while the concentration of Hydroxy propyl cellulose (HPC SSL), Kollicoat IR, and sonication time were considered as independent variables. According to the study, every independent variable significantly affected the dependent variables ($p < 0.05$). The size of the particle GLMP-NP ranged between 159 (F2) to 505 nm (F8) while EE varied from 32 (F8) to 75% (F2). The DR of the GLMP-NP observed at 10 min ranged between 35 (F8) to 100% (F2). A significant enhancement in dissolution rate was observed in GLMP-NPs (F1-F8) in comparison to pure GLMP. It was discovered that pure GLMP dissolved in 27.25 ± 6.8 µg/mL of double-distilled water, while GLMP-NP exhibited 3.50 to 6.58-fold enhancement in saturation solubility. FTIR and DSC analysis revealed excellent compatibility between GLMP and excipients. XRD study confirmed the amorphous nature of the nanoparticles while SEM analysis revealed a smooth surface. In conclusion, this study demonstrates the substantial improvement in dissolution rate and solubility of pure GLMP when formulated as nanoparticles.

Keywords: Glimepiride, Nanoparticles, Nanosuspension, Solubility, Ultrasonication, Precipitation.

International Journal of Drug Delivery Technology (2023); DOI: 10.25258/ijddt.13.4.21

How to cite this article: Padmnabh, Bhatt DC. Development, Optimization and Characterization of Glimepiride Nanosuspension with Improved Solubility and Dissolution. International Journal of Drug Delivery Technology. 2023;13(4):1248-1257.

Source of support: Nil.

Conflict of interest: None

INTRODUCTION

It is indeed a common observation in the field of pharmaceutical development that several active pharmaceutical ingredients (APIs) exhibit poor bioavailability and water solubility.[1] This challenge is widely recognized and has significant implications for drug development. The solubility and bioavailability of newly synthesized drug molecules are critical factors that can significantly impact the success of drug development.[2] Many newly synthesized drug molecules have poor aqueous solubility, which can limit their absorption in the gastrointestinal tract. Poor solubility can result in low bioavailability, making it challenging to achieve therapeutic concentrations in the bloodstream.[3] Various approaches including prodrugs, salt formation, co-solvents, complexation, and modification of crystal forms are used in solubility, dissolution and bioavailability enhancement.

NPs is highly popular in the pharmaceutical field as a potential technique to increase solubility of the weakly soluble medicines. The fascinating characteristics and functional benefits of NPs have captured the attention of researchers and scientists across diverse domains, including medicine, biology, and engineering. These properties encompass attributes like size, shape, durability, strength, extended action duration, and their remarkable adaptability to house a wide array of molecules.[4] This multidisciplinary interest underscores the versatile potential of NPs in various applications within the realms of medicine and biology. Nanoparticles offer an exceptional surface-to-mass ratio, surpassing that of conventional particles and materials.[5] This unique feature not only facilitates catalytic reactions but also enables the absorption and transportation of diverse compounds. In the fields of medicine and biology, the utility of nanoparticles extends across numerous fronts.[6] They have revealed promise in a multitude of applications, with a primary emphasis on revolutionizing drug delivery. NPs play a pivotal role in augmenting drug solubility, enhancing bioavailability, and finely tuning controlled and sustained release profiles. Their adaptability and versatility make them indispensable in this sphere.[7]

**Author for Correspondence: padmanabhkm@gmail.com*

To produce drug particles at the nanoscale or micronized level, antisolvent precipitation has emerged as a highly effective method. In one approach, API is allowed to dissolve in the solvent phase and immediately introduced into an antisolvent phase, resulting in the precipitation of the drug. This method, recognized as a bottom-up approach, is widely employed in the creation of nanosuspensions due to its simplicity and cost-effectiveness.[8,9] However, this approach is not without its challenges. It is associated with the issues related to maintaining precise particle sizes, achieving stability post-precipitation, and scaling up production batches.[10, 11] To address these challenges, ultrasonication, when combined with the precipitation process, emerges as a powerful strategy. This synergistic approach effectively enhances particle size reduction.

Glimeperide (GLMP) is an oral sulfonylurea medication that is frequently used in the treatment of diabetes.[12] Notably, GLMP is known for its potent hypoglycemic effects and a low risk of systemic toxicity.[13] Considering the Biopharmaceutical Classification System (BCS), it comes under class II medication due to high permeability and lower solubility.[14] However, the limited aqueous solubility of GLMP presents significant challenges. It hinders the preparation of effective oral pharmaceutical formulations, results in a suboptimal dissolution profile, and ultimately leads to low bioavailability.[15] The oral absorption of such weakly water-soluble medications relies heavily on their dissolution rate within the gastrointestinal tract fluids.[16] Hence, the primary objective of the work is to enhance aqueous solubility and dissolution of GLMP using a nanoparticulate drug delivery system.

MATERIALS AND METHODS

GLMP had been received as a sample gift from Tiruvision Medicare, Baddi. Sodium lauryl sulphate (SLS) was obtained from Labogens and hydroxy propyl cellulose SSL (HPC SSL) from Nisso. Kollicoat was gift sample from BASF India Limited. Acetone was purchased from Ibuychemikals. Methanol was obtained from Labogens. Analytical-grade chemicals and reagents were used for all other purposes.

Experimental Design by 3-factor, 2-level full factorial

Preliminary experiments demonstrated that drug release, encapsulation efficiency, and particle size from nanoparticles were influenced by the concentration of HPC, Kollicoat, and sonication time. So, these three parameters are regarded as independent variables. The nanoparticles were optimized and the impact of independent factors on dependent ones was differential levels are depicted in Table 1.

Formulation of Glimepiride Nanoparticles (GLMP-NP)

Glimepiride nanoparticles (GLMP-NP) was manufactured using the precipitation–ultrasonication method.[17] Accurately weighed 50 mg of GLMP was dissolved in a beaker containing 6 mL solution of acetone and methanol (1:1) and considered as organic phase. In another beaker, 15 mL double distilled water, required quantities of HPC (75, 150 mg), Kollicoat (100, 150 mg), and SLS (1.80 mg) were dissolved under magnetic stirring and solution was pre-cooled up to 4°C The drug-containing organic phase was gradually introduced to the antisolvent phase containing polymers and surfactant at 1500 rpm under magnetic stirring. Later, to reduce the size of NPs, ultrasonication done for 10 and 15 minutes. The resulting nanosuspension was allowed to centrifuge at 5,000 rpm for 20 minutes. With caution, supernatant solution was decanted and sedimented NPs were dried for 48 hours at 40°C in an oven. Prior to further examination, the dried nanoparticles were preserved in amber-colored glass vials and placed in a desiccator. The different batches are depicted in Table 2.

Table 1: Levels and variables

Variables	*-1 level*	*+1 Level*
Independent variables		
A= HPC (mg)	75	150
B= Kollicoat (mg)	100	150
C=Sonication Time (minutes)	10	15
Dependent variables		
Y1= Particle size		
Y2 = EE		
Y3= %DR at 10 minutes		

Characterization of GLMP-NP

Particle size and zeta potential

Prior to analysis, the dehydrated GLMP-NP was immersed in double-distilled water and sonicated for a duration of one minute. With Zetasizer, the zeta potentials and particle sizes were determined (Malvern instruments ZS 90) at room temperature.[18]

Drug entrapment efficiency (EE)

Non-encapsulated GLMP was determined using the supernatant that was left behind after centrifugation. Using ultra violet spectroscopy set at 228 nm, samples were examined. The following formulas were used to compute the NPs' entrapment efficiency (EE).[19]

%E.E = Total drug-free drug /Total drug x 100

Drug release study

For pure GLMP and GLMP-NP, an in vitro release investigation was conducted using 900 mL of pH 7.8 phosphate buffer. GLMP and GLMP-NP were dispersed separately in to 3 mL pH 7.8 phosphate buffer and this dispersion was filled in a dialysis tube and tied from both ends. These tubes then dispersed in dissolution test apparatus containing release media maintaining a 37 ± 0.5°C temperature while the paddles are rotating at 75 rpm. After a duration of 0, 5, 10, 15, 30, 45, and 60 minutes, 5 mL sample aliquots were obtained and. Every time, release media was replaced with 5 mL media. At 228 nm, the drug's concentration was determined by UV spectroscopy.[20]

Saturation solubility

To make sure the drug reached the saturation point, an excess of pure GLMP was added to 5 mL of water. By adding an excessive amount of distilled water, a similarly saturated

solution of GLMP-NP was also produced. These solutions underwent a 24-hour mechanical shaking period at 37°C, followed by a 3-minute centrifugation at 10,000 rpm. After that, the saturated solutions were diluted to the appropriate concentration. At 228 nm, the drug's concentration was determined by UV spectroscopy.[21]

Shape and surface morphology

Surface morphology and shape was investigated using scanning electron microscopy (Jeol Ltd Japan). At 15.0 kV of acceleration, the working distance was kept between 8.6 and 8.8 mm. By applying a gold coating, the nanoparticles became electrically conductive. A brass tub was used to mount these gold-coated nanoparticles using double-sided adhesive tape. The ion sputter was kept at 5 Pa vacuum throughout the entire process.[19]

Infrared spectroscopy using the fourier transform

In order to investigate potential interactions between GLMP and the excipients used in the NP as well as the stability of the drug during this process, FTIR spectroscopy was conducted.[19] The analysis was carried out using the potassium bromide disc method, whereby samples of approximately palletized under vacuum, 2 to 3 mg of the mixture were combined with KBr, and analyzed using a FTIR spectrophotometer (PerkinElmer, US) over a 4000 to 400 cm^{-1} range.

Differential scanning calorimeter

DSC (TA instruments, US) was performed to confirm any potential interactions between GLMP and the excipients used in the NP loading process and to assess the drug's ability to withstand this process. Samples weighing 5 mg were heated at 100°C/min rate in flat-bottomed aluminum pans in the presence of nitrogen with a 30 mL/min flow rate over a temperature range of 33 to 300°C. Aluminum pans that were empty served as a reference.[19]

Analysis using X-ray diffraction

GN, physical mixtures, and pure drugs were all subjected to XRD studies using Malvern PANalytical, UK.[19]

RESULTS AND DISCUSSION

Statistical Analysis of Particle Size (Y1)

Nanoparticle size can significantly influence the efficacy, safety, and pharmacokinetics of the delivered drugs. The size of NPs typically ranges from 1 to 1000 nm, and this size range offers several advantages.[22] Nanoparticles can enhance drug solubility, particularly for hydrophobic drugs, improving their bioavailability. They also provide drug stability by shielding drugs from degradation processes.[23] Moreover, nanoparticle size influences biodistribution, facilitating targeted drug delivery to specific tissues or cells while reducing exposure to healthy ones. Nanoparticles can prolong drug circulation in the bloodstream, benefiting from the increase in permeability and retention, particularly in tumors. Additionally, controlled drug release from nanoparticles reduces toxicity and enhances cellular uptake, optimizing therapeutic efficacy. Finally, nanoparticle size and surface properties can be engineered to tailor drug release kinetics, customizing delivery profiles for specific applications.[24]

Table 2: Different batches of GLMP NPs

Batches	*Factor*		
	A (HPC, mg)	*B (Kollicoat, mg)*	*C (Sonication time, min)*
F1	-1	+1	-1
F2	+1	+1	+1
F3	-1	+1	+1
F4	+1	-1	+1
F5	+1	-1	-1
F6	-1	-1	+1
F7	+1	+1	-1
F8	-1	-1	-1

Table 3 displays all of the formulations' particle size data as well as the dependent variables' coded levels.

The particle size of the GLMP-NP was ranged between 159 (F2) to 505 nm (F8). F2 NPs showed the lowest particle size than other formulations. The distribution of particle size F2 is presented in Figure 1. An excellent PDI of 0.251 was observed for F2. From Figure 2, a zeta potential of -26.6 mV was observed that lies within an acceptable range of -30 to +30 mV indicating excellent stability of nanosuspension.

The wide range of particle sizes that were seen indicates that the independent factors had a greater impact on the particle sizes. Table 4 shows the diagnostic case statistics of particle size with actual and expected values.

The study reveals a clear relationship between particle size and the concentrations of HPC SSL, Kollicoat IR, and sonication time. The lower particle size was observed with higher levels of independent variables and vice versa. This relationship and the impact of the independent variables on particles are graphically represented in Figure 3.

The final polynomial equation for particle size (Y1) in coded factors can be presented below

$$(Y1) = +325.13 - 76.13A - 85.38B - 58.63C + 47.12ABC$$

Particle size is denoted by Y1, HPC concentration by A, Kollicoat concentration by B, and sonication time by C in the equation above. The model is considered statistically significant when $p < 0.05$. In our experiment variables A, B, C, and ABC were found to be statistically significant (Table 5). Based on an F-value of 88.38, the model was also found statistically significant (Table 5). F-value this large could only be the result of noise in 0.19% of cases. There is less than 0.2 discrepancy between the adjusted R^2 of 0.9804 and the expected R^2 of 0.9402 (Table 5). The signal-to-noise ratio is assessed. Ideally, there should be a ratio higher than 4. The ratio of 21.251 in our model suggested an adequate signal.

Statistical Analysis of EE (Y2)

EE is a pivotal factor in nanoparticulate technology. It quantifies the percentage of drug molecules effectively enclosed within nanoparticles, with higher efficiency equating to more precise drug delivery to the target site, essential

Table 3: Results of particle size with levels of independent variables

Batches	Factor			Particle size
	A (HPC SSL, mg)	*B (Kollicoat IR, mg)*	*C (Sonication time, min)*	*Y1 (nm)*
F1	-1	+1	-1	400
F2	+1	+1	+1	159
F3	-1	+1	+1	220
F4	+1	-1	+1	207
F5	+1	-1	-1	450
F6	-1	-1	+1	480
F7	+1	+1	-1	180
F8	-1	-1	-1	505

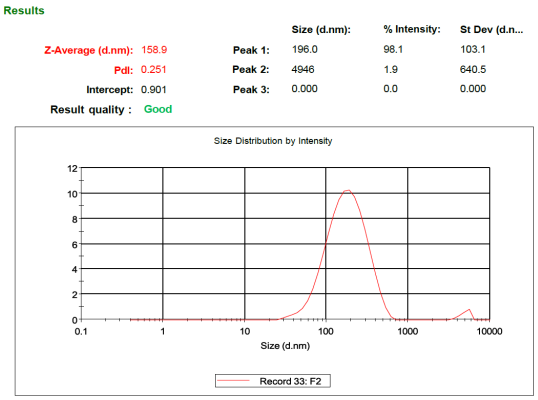

Figure 1: Distribution of particle sizes of the F2 GLMP-NPs

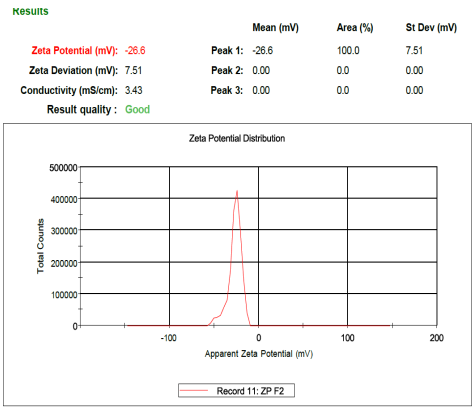

Figure 2: Zeta potential of F2 formulation

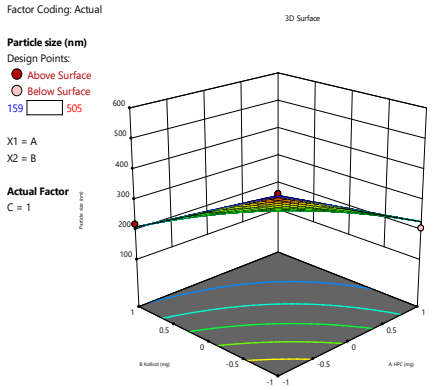

Figure 3: 3D surface responses of HPC and Kollicoat at a higher level of sonication time on particle size

for achieving the desired therapeutic effects while reducing wastage. This optimization is economically significant, particularly for costly pharmaceuticals, as it ensures a greater portion of the drug serves therapeutic purposes instead of being lost during formulation, ultimately reducing production expenses.[25] Furthermore, efficient encapsulation can minimize drug toxicity by decreasing the concentration of free drugs in the bloodstream, thereby mitigating potential side effects and enhancing treatment safety. Encapsulation efficiency also plays a pivotal role in controlling drug release kinetics, enabling sustained and predictable drug release over time, and resulting in consistent therapeutic outcomes.[26] Additionally, it allows for tailoring nanoparticle formulations to meet specific drug and medical condition requirements. Lastly, high encapsulation efficiency helps maintain drug stability.[27] EE directly impacts the effectiveness, safety, and economic feasibility of drug delivery. Maximizing the amount of drug that can be encapsulated within nanoparticles ensures that a larger portion of the drug reaches the intended target, resulting in improved therapeutic outcomes and more efficient use of pharmaceutical resources.[28]

Table 6 shows the EE results for each formulation along with the coded levels of the dependent variables.

The EE of the GLMP-NP was ranged between 32 (F8) to 75% (F2). F2 nanoparticles showed the highest EE than other formulations. The diagnostic case statistics of particle size with actual and expected values are depicted in Table 7.

Table 4: An analysis of particle size diagnostic case statistic

Run order	*Actual value*	*Predicted value*	*Residual*	*Leverage*	*Internally studentized residuals*	*Externally studentized residuals*	*Cook's distance*	*Influence on fitted value dffits*
1	400.00	421.63	-21.63	0.625	-1.715	-9.922	0.980	-12.810
2	159.00	152.12	6.88	0.625	0.545	0.469	0.099	0.605
3	220.00	210.13	9.87	0.625	0.783	0.717	0.204	0.925
4	207.00	228.63	-21.63	0.625	-1.715	-9.922	0.980	-12.810
5	450.00	440.13	9.87	0.625	0.783	0.717	0.204	0.925
6	480.00	475.13	4.87	0.625	0.387	0.324	0.050	0.418
7	180.00	175.13	4.87	0.625	0.387	0.324	0.050	0.418
8	505.00	498.13	6.87	0.625	0.545	0.469	0.099	0.605

Table 5: ANOVA for particle size

Source	*Sum of Squares*	*df*	*Mean Square*	*F-value*	*p-value*	
Model	1.499	4	37483.13	88.38	0.0019	significant
A-HPC	46360.13	1	46360.13	109.31	0.0019	
B-Kollicoat	58311.13	1	58311.13	137.49	0.0013	
C-Sonication	27495.13	1	27495.13	64.83	0.0040	
ABC	17766.12	1	17766.12	41.89	0.0075	
Residual	1272.38	3	424.13			
Cor Total	1.512	7				
Statistics						
Std. Dev.	20.59		R^2	0.9916		
Mean	325.13		Adjusted R^2	0.9804		
CV%	6.33		Predicted R^2	0.9402		
	Adeq Precision		21.2515			

Table 6: Results of EE with levels of independent variables

Batches	*Factor*			*EE*
	A (HPC SSL, mg)	*B (Kollicoat IR, mg)*	*C (Sonication time, min)*	*Y2 (nm)*
F1	-1	+1	-1	48
F2	+1	+1	+1	75
F3	-1	+1	+1	60
F4	+1	-1	+1	65
F5	+1	-1	-1	45
F6	-1	-1	+1	40
F7	+1	+1	-1	69
F8	-1	-1	-1	32

The study reveals a direct relation between EE and independent variables. The higher EE was observed at a higher level of the independent variables. Higher polymer concentrations provided more scope to encapsulate the maximum amount of drug within the polymeric matrix. The batches with lower levels showed the minimum EE. This relationship illustrates how the independent variables affect EE are graphically represented in Figure 4.

The final polynomial equation for EE (Y2) in coded factors can be presented below

(Y2) = +54.25 +9.25A+8.75B+5.75C-2.25ABC

A *p-value* below 0.0500 indicated significant model. The variables A, B, C, and ABC are statistically significant in this instance. Values higher than 0.0500 signify the lack of significance for the model terms in this case the combined effect of ABC is not statistically significant (p = 0.0780) (Table 8). The model is significant, as indicated by the F-value of 68.66 (Table 8). Only 0.28% of occurrences with an F-value this high could be the consequence of noise. There is less than 0.2 discrepancy between the adjusted R^2 of 0.9748 and the expected R^2 of 0.9232 (Table 8). The signal-to-noise ratio was assessed. Ideally, there should be a ratio greater than 4. The 22.520 ratio in our model suggested a sufficient signal.

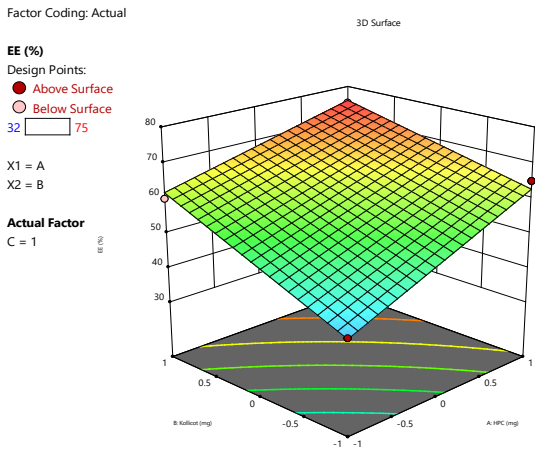

Figure 4: 3D surface responses of HPC and Kollicoat at a higher level of sonication time on EE

Statistical Analysis of DR at 10 Minutes (Y3)

Enhancing drug dissolution rates through nanoparticle-based formulations is a pivotal technique in pharmaceuticals, particularly for poorly water-soluble drugs like GLMP. This method involves encapsulating drug molecules within nanoparticles with enhanced solubility. Poorly soluble drugs often encounter absorption challenges in the gastrointestinal tract, resulting in limited therapeutic efficacy. Nanoparticles, by increasing the surface area available for drug molecules to interact with the surrounding solvent, substantially enhance solubility.[29] Consequently, a more significant proportion of the administered dose can be efficiently absorbed into the bloodstream, leading to heightened bioavailability and improved therapeutic outcomes.[30] Furthermore, nanoparticle-based formulations promote rapid action, which proves advantageous for acute conditions or drugs requiring rapid therapeutic levels. They also reduce variability in drug absorption compared to traditional formulations, offering more predictable and consistent therapeutic effects across different individuals. Lower dosing requirements are often achievable with improved solubility, reducing the risk of side effects and

Table 7: Diagnostic statistics of EE

Run order	*Actual value*	*Predicted value*	*Residual*	*Leverage*	*Internally studentized residuals*	*Externally studentized residuals*	*Cook's distance*	*Influence on fitted value DFFITS*
1	48.00	45.75	2.25	0.625	1.521	2.598	0.771	3.354
2	75.00	75.75	-0.7500	0.625	-0.507	-0.433	0.086	-0.559
3	60.00	61.75	-1.75	0.625	-1.183	-1.323	0.467	-1.708
4	65.00	62.75	2.25	0.625	1.521	2.598	0.771	3.354
5	45.00	46.75	-1.75	0.625	-1.183	-1.323	0.467	-1.708
6	40.00	39.75	0.2500	0.625	0.169	0.139	0.010	0.179
7	69.00	68.75	0.2500	0.625	0.169	0.139	0.010	0.179
8	32.00	32.75	-0.7500	0.625	-0.507	-0.433	0.086	-0.559

Table 8: ANOVA for a specific EE

Source	*Sum of squares*	*df*	*Mean square*	*F-value*	*p-value*	
Model	1602.00	4	400.50	68.66	0.0028	significant
A-HPC	684.50	1	684.50	117.34	0.0017	
B-Kollicoat	612.50	1	612.50	105.00	0.0020	
C-Sonication	264.50	1	264.50	45.34	0.0067	
ABC	40.50	1	40.50	6.94	0.0780	
Residual	17.50	3	5.83			
Cor Total	1619.50	7				
Statistics						
Std. Dev.	2.42		R^2	0.9892		
Mean	54.25		Adjusted R^2	0.9748		
CV%	4.45		Predicted R^2	0.9232		
	Adeq Precision		22.5201			

Table 9: Results of drug release at 10 minutes with levels of independent variables

Batches	*Factor*			*DR at 10 minutes*
	A (HPC, mg)	*B (Kollicoat, mg)*	*C (Sonication time, min)*	*Y3 (%)*
F1	-1	+1	-1	55
F2	+1	+1	+1	100
F3	-1	+1	+1	72
F4	+1	-1	+1	80
F5	+1	-1	-1	50
F6	-1	-1	+1	42
F7	+1	+1	-1	85
F8	-1	-1	-1	35

production costs. Overall, nanoparticle-mediated dissolution rate enhancement holds substantial promise in overcoming the solubility limitations of drugs and improving their therapeutic potential.[31] In Table 9, coded levels of the dependent variables are displayed alongside the drug release outcomes for each formulation.

The DR of the GLMP-NP observed at 10 min ranged between 35 (F8) to 100 % (F2). F2 nanoparticles showed rapid DR as compared to other batches. The higher EE and smaller particle size of the F2 nanoparticles might be responsible for the rapid release of GLMP from nanoparticles. The diagnostic case statistics of particle size with actual and predicted values are depicted in Table 10.

The study reveals a clear relationship between DR and the concentrations of HPC, Kollicoat, and sonication time. The rapid DR was observed with higher levels of independent variables while DR was found to be decreased with lower levels. This relationship and the impact of the independent variables on drug release are graphically represented in Figure 5.

The final polynomial equation for DR (Y3) in coded factors can be presented below

$$(Y3) = +64.88 +13.88A+13.13B+8.62C-3.12ABC$$

The model is considered statistically significant when $p<0.05$. In our experiment variables A, B, and C were found to be statistically significant. The combined effect of ABC is not statistically significant ($p = 0.1457$) (Table 11). The model is significant, as indicated by its F-value of 43.89 (Table 11). An F-value this large could only be the result of noise in 0.54% of cases. The discrepancy between the adjusted R^2 of 0.9608 and the expected R^2 of 0.8805 is less than 0.2, indicating a satisfactory agreement (Table 11). The signal-to-noise ratio is measured with adeq precision. Ideally, there should be a ratio higher than 4. In our model ratio of 18.178 suggests an adeq signal.

Table 10: DR diagnostic statistics

Run order	*Actual value*	*Predicted value*	*Residual*	*Leverage*	*Internally studentized residuals*	*Externally studentized residuals*	*Cook's distance*	*Influence on fitted value dffits*
1	55.00	52.38	2.63	0.625	0.948	0.924	0.299	1.193
2	100.0	97.38	2.63	0.625	0.948	0.924	0.299	1.193
3	72.00	75.88	-3.88	0.625	-1.399	-1.938	0.652	-2.501
4	80.00	77.38	2.63	0.625	0.948	0.924	0.299	1.193
5	50.00	53.88	-3.88	0.625	-1.399	-1.938	0.652	-2.501
6	42.00	43.38	-1.38	0.625	-0.496	-0.423	0.082	-0.546
7	85.00	86.38	-1.38	0.625	-0.496	-0.423	0.082	-0.546
8	35.00	32.38	2.63	0.625	0.948	0.924	0.299	1.193

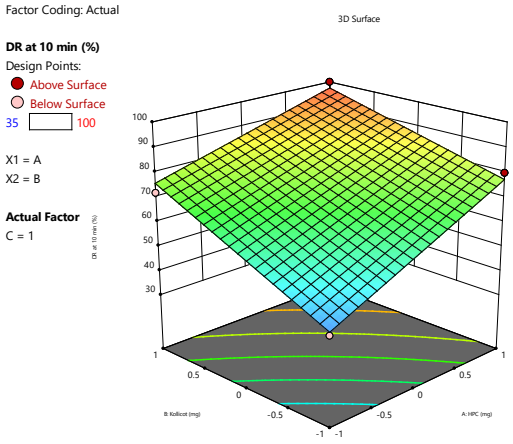

Figure 5: 3D surface responses of HPC and Kollicoat at a higher level of sonication time on DR

Comparative Drug Release Profile

The comparative DR profile of pure GLMP, GLMP-NP (F1 to F8) formulation is presented in Figure 6.

A significant enhancement in dissolution rate was observed in GLMP-NPs (F1-F8) in comparison to pure GLMP and marketed formulations. Out of all NP formulations, the F2 formulation showed 100% release within 10 minutes. Pure GLMP showed nearly 35% release over 60 minutes. The

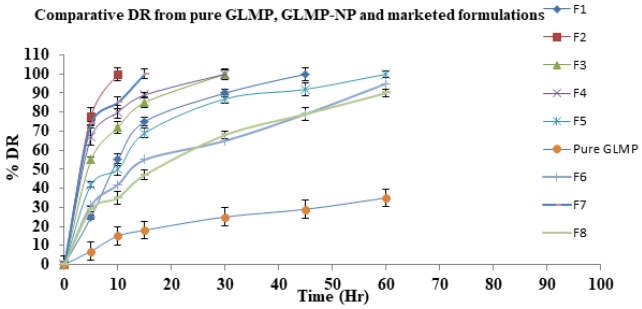

Figure 6: Comparative *in-vitro* DR of pure GLMP, GLMP-NP (F1 to F8) GLMP formulation in phosphate buffer pH 7.8

reduced nanoparticulate size and higher EE of GLMP-NPs are responsible for the rapid dissolution of the NPs.

Saturation Solubility

Drastic enhancement in the solubility of the GLMP was observed when it was formulated as nanoparticles. The solubility of pure GLMP in water was 27.25 ± 6.8 µg/mL, while GLMP-NP exhibited 3.50 to 6.58-fold enhancement in saturation solubility as compiled in Table 12.

The F2 formulation showed the highest (6.58-fold) enhancement in solubility in comparison to pure GLMP and other NP formulations (Figure 7). A high surface area-to-volume ratio offers more interaction points for drug molecules

Table 11: ANOVA for a specified DR

Source	*Sum of Squares*	*df*	*Mean Square*	*F-value*	*p-value*	
Model	3591.50	4	897.88	43.89	0.0054	Significant
A-HPC	1540.12	1	1540.12	75.28	0.0032	
B-Kollicot	1378.12	1	1378.12	67.36	0.0038	
C-Sonication	595.12	1	595.12	29.09	0.0125	
ABC	78.13	1	78.13	3.82	0.1457	
Residual	61.38	3	20.46			
Cor Total	3652.88	7				
Statistics						
Std. Dev.	4.52		R^2	0.9832		
Mean	64.88		Adjusted R^2	0.9608		
CV%	6.97		Predicted R^2	0.8805		
	Adeq Precision		18.1777			

Table 12: Saturation solubility of pure GLMP and GLMP-NP with fold enhancements

S. No.	*Formulation*	*Solubility (µg/mL)*	*Fold enhancement*
1	Pure GLMP	27.25 ± 6.8	NA
2	F1	127.11 ± 7.8	4.66
3	F2	179.26 ± 5.5	6.58
4	F3	140.27 ± 7.6	5.15
5	F4	155.12 ± 8.5	5.69
6	F5	110.12 ± 10.5	4.04
7	F6	100.21 ± 12.5	3.68
8	F7	160.22 ± 10.8	5.88
9	F8	95.26 ± 7.9	3.50

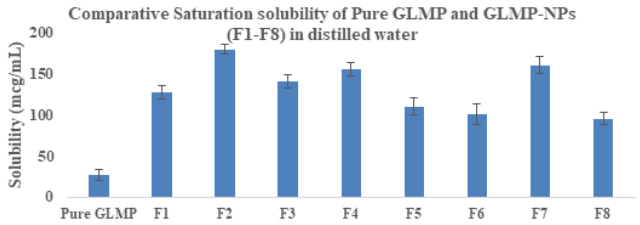

Figure 7: Comparative saturation solubility of pure GLMP and GLMP-NP (F1-F8) in water

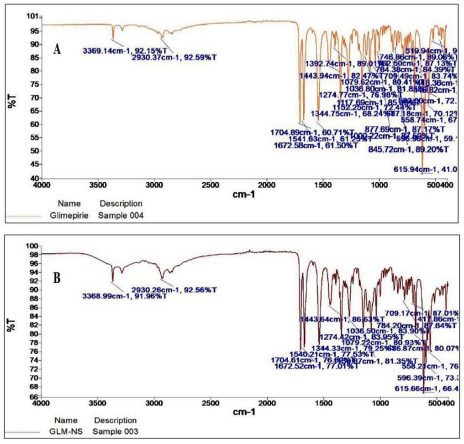

Figure 8: FTIR spectra of (A): Pure GLMP and (B): optimized GLMP-NP (F2)

to engage with water molecules, facilitating greater dissolution. At the nanoscale, materials often exhibit size-dependent properties, which can alter surface energies and charges, further promoting drug-water interactions.[32] The minimum size of the nanoparticles shortens the diffusion distance for water molecules around the drug, breaking intermolecular forces that hinder dissolution.[33] Certain nanoparticle formulations can even convert drugs from crystalline to amorphous states, known for their improved water solubility. Surface modifications with hydrophilic coatings or surfactants enhance nanoparticle-water interactions and prevent drug aggregation. Collectively, these mechanisms bolster the bioavailability and solubility of weakly soluble drugs, addressing a significant challenge in pharmaceutical development.

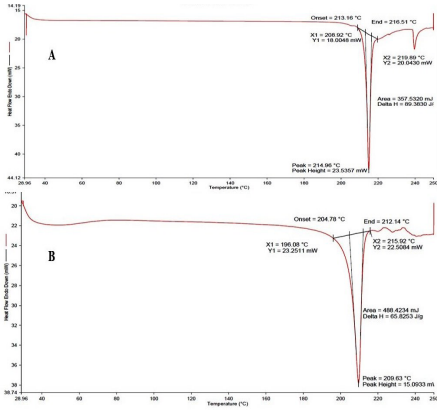

Figure 9: DSC thermograms of (A): Pure GLMP and (B): optimized GLMP-NP (F2)

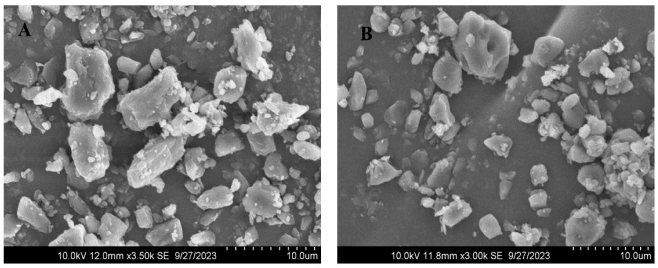

Figure 10: Surface morphology of A: Pure GLMP and B: GLMP-NP

FTIR Analysis

The characteristic FTIR peaks observed in GLMP can be seen in Figure 8 (A). GLMP has a secondary amine group, so a weak but characteristic peak in the range of 3200–3369.14 cm^{-1} was observed due to N-H stretching. A strong peak around 1704 cm^{-1} was discovered, suggesting the presence of the carbonyl (C=O Stretch) group in GLMP. Stretching vibrations of C-H are suggested by the peak at 2930 cm^{-1} area, which might be due to various sources such as alkanes, alkenes, and aromatic rings within the compound. C-C Stretch (Aromatic Rings): GLMP contains aromatic rings, so peaks at 1443 cm^{-1} correspond to the characteristic of C-C stretching vibrations in aromatic structures. GLMP includes a sulfur atom, a strong peak at 615 cm^{-1} was observed indicating the C-S stretching vibration. Similar characteristic peaks were also observed in the optimized formulation of GLMP as shown in Figure 8(B). These observations indicated strong compatibility between GLMP and excipients used.

DSC Analysis

In pure GLMP's DSC a prominent endothermic peak at 214.96°C was observed, which was within range of melting temperature of 212 to 216°C and indicates that it is crystalline (Figure 9A). In contrast, GLMP-loaded nanoparticles showed an endothermic peak at 209.63°C. This slight shifting of the peak indicated the amorphization of the drug within the polymeric matrix **(**Figure 9B). This disappearance of the endothermic peak at 214.96°could be attributed to the encapsulation of GLMP within the polymeric matrix.

Table 13: Optimized independent variables for the most preferred formulation and percent bias estimation by comparison of the optimized GLMP-NPs observed and anticipated values

Independent variables	*A (HPC, mg)*	*B (Kollicoat, mg)*	*C (Sonication time, min)*	*Desirability*
GLMP-NP	150	150	15	0.986
S. No	*Dependent variables*	*Predicted*	*Actual*	*%Bias*
1	Y1= Particle size	152.125	151.24	0.5817
2	Y2 = EE	75.75	74.47	1.68
3	Y3= % DR at 10 minues	97.375	96.9	0.48

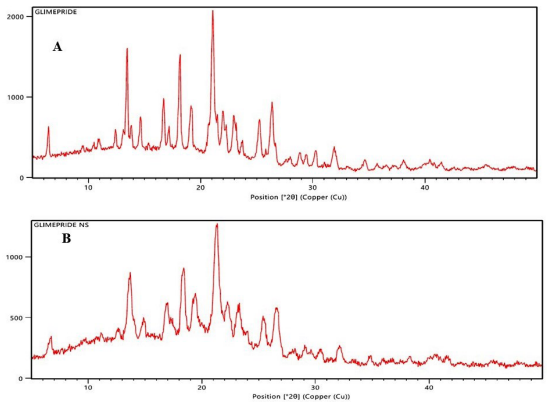

Figure 11: XRD of (A): Pure GLMP and (B): optimized GLMP-NP (F2)

Surface Properties of NPs

Using a scanning electron microscope (SEM), the morphology of both GLMP and produced GLMP-NP was studied. The surface of the pure GLMP was found to be irregular, bigger irregularly shaped particles were observed with clusters in different areas (Figure 10A). The surface was found to be smooth without cracks in the case of GLMP-NPs. The GLMP-NPs were found to be slightly prismatic, irregular and rod-shaped crystals (Figure 10B). Also, very few tiny particles were also detectable forming a cluster to give rise to big particle appearance.

Analysis of XRD

Figure 2 shows the XRD data of plain GLMP (Figure 11A). Numerous distinct, strong and sharp peaks were observed at diffraction angle (2θ) of 10.9327°, 12.4005°, 13.4236°, 14.6180°, 15.9174°, 18.1153°, 19.1306°, 21.0581°, 22.9619°, 25.2037°, and 26.3216°. These sharp peaks were the indicative of crystalline nature of the pure GLMP. In case of GLMP-NP, slightly reduced intensity peaks were observed at diffraction angles (2θ) of 13.6399°, 16.9310°, 19.3686°, 21.2523°, 21.3428°, 23.2098°, 25.4233°, and 26.5299° (Figure 11 B). These reduced intensity peaks of GLMP-NP showed the amorphous nature of the developed nanoparticles.

Optimal parameters for formulation and verification of the model

Through numerical optimization, the ideal formulation variable values were determined, with a maximum desirability of 0.986 (Table 13). A least percentage of bias was observed between predicted and experimental result. This demonstrated the model's reliability and reasonable.

CONCLUSION

In this research, GLMP nanoparticles-suspension (NPs) were developed to enhance their solubility and dissolution. The particle size range for GLMP-NPs was found to be 159 to 505 nm, EE from 32 to 75%, and 10-minute drug release from 35 to 100%, outperforming pure GLMP. Solubility increased from 3.50 to 6.58-fold, showcasing the potential for enhanced GLMP therapy in type II diabetes. In summary, this study demonstrates a substantial enhancement in solubility as well as dissolution of pure GLMP when formulated as nanoparticles. These findings hold the potential to enhance the therapeutic effectiveness and bioavailability of GLMP, potentially leading to more efficient treatments for individuals with type II diabetes mellitus.

REFERENCES

1. Moinuddin, Neekhra S, Swarnkar SK, Gupta P, Gupta D, Khunteta A, Kaushik U, Ahmad S. Dasatinib and Hesperidin Loaded Nano Formulation and Preclinical Evaluation for Anticancer Activity. International Journal of Pharmaceutical Quality Assurance. 2023;14(3):579-586. https://doi.org/10.25258/ijpqa.14.3.20
2. Arnott JA, Planey SL. The influence of lipophilicity in drug discovery and design. Expert opinion on drug discovery. 2012 Oct 1;7(10):863-75. https://doi.org/10.1517/17460441.2012.714363
3. Kolimi P, Narala S, Youssef AA, Nyavanandi D, Dudhipala N. A systemic review on development of mesoporous nanoparticles as a vehicle for transdermal drug delivery. Nanotheranostics. 2023;7(1):70. DOI: 10.7150/ntno.77395
4. Shirman E, Shirman T, Shneidman AV, Grinthal A, Phillips KR, Whelan H, Bulger E, Abramovitch M, Patil J, Nevarez R, Aizenberg J. Modular design of advanced catalytic materials using hybrid organic–inorganic raspberry particles. Advanced Functional Materials. 2018 Jul;28(27):1704559. https://doi.org/10.1002/adfm.201704559
5. Zottel A, Videtič Paska A, Jovčevska I. Nanotechnology meets oncology: nanomaterials in brain cancer research, diagnosis and therapy. Materials. 2019 May 15;12(10):1588. https://doi.org/10.3390/ma12101588
6. Thorat S, Tare M. Formulation and Evaluation of Quercetin Loaded Nanosponges of Abiraterone Acetate. International Journal of Pharmaceutical Quality Assurance. 2023;14(3):648-655. https://doi.org/10.25258/ijpqa.14.3.32
7. Khairnar SV, Pagare P, Thakre A, Nambiar AR, Junnuthula V, Abraham MC, Kolimi P, Nyavanandi D, Dyawanapelly S. Review on the scale-up methods for the preparation of solid lipid nanoparticles. Pharmaceutics. 2022 Sep 6;14(9):1886. https://doi.org/10.3390/pharmaceutics14091886
8. Agarwal P, Vasudha B. Preparation and Evaluation of Primidone

Solid Lipid Nanoparticle for Alleviating Seizure Activity in Wistar Rats. International Journal of Drug Delivery Technology. 2023;13(3):919-925. https://doi.org/10.25258/ijddt.13.3.24

9. Alshweiat A, Katona G, Csóka I, Ambrus R. Design and characterization of loratadine nanosuspension prepared by ultrasonic-assisted precipitation. European Journal of Pharmaceutical Sciences. 2018 Sep 15; 122:94-104. https://doi.org/10.1016/j.ejps.2018.06.010
10. Alshweiat A, Katona G, Csóka I, Ambrus R. Design and characterization of loratadine nanosuspension prepared by ultrasonic-assisted precipitation. European Journal of Pharmaceutical Sciences. 2018 Sep 15; 122:94-104. https://doi.org/10.1016/j.ejps.2018.06.010
11. De Castro ML, Priego-Capote F. Ultrasound-assisted crystallization (sonocrystallization). Ultrasonics sonochemistry. 2007 Sep 1;14(6):717-24. https://doi.org/10.1016/j.ultsonch.2006.12.004
12. González-Ortiz M, Guerrero-Romero JF, Violante-Ortiz R, Wacher-Rodarte N, Martínez-Abundis E, Aguilar-Salinas C, Islas-Andrade S, Arechavaleta-Granell R, González-Canudas J, Rodríguez-Morán M, Zavala-Suárez E. Efficacy of glimepiride/metformin combination versus glibenclamide/metformin in patients with uncontrolled type 2 diabetes mellitus. Journal of Diabetes and its Complications. 2009 Nov 1;23(6):376-9. https://doi.org/10.1016/j.jdiacomp.2008.09.002
13. Gill B, Kaur T, Kumar S, Gupta GD. Formulation and evaluation of glimepiride solid dispersion tablets. Asian Journal of Pharmaceutics (AJP). 2010;4(3). https://doi.org/10.22377/ajp.v4i3.221
14. Wagh VT, Jagtap VA, Shaikh TJ, Nandedkar SY. Formulation and evaluation of glimepiride solid dispersion tablets for their solubility enhancement. Journal of Advanced Scientific Research. 2012 Nov 10;3(04):36-41.
15. Ning X, Sun J, Han X, Wu Y, Yan Z, Han J, He Z. Strategies to improve dissolution and oral absorption of glimepiride tablets: solid dispersion versus micronization techniques. Drug development and industrial pharmacy. 2011 Jun 1;37(6):727-36. https://doi.org/10.3109/03639045.2010.538061
16. Sharma M, Sharma R, Jain DK, Saraf A. Enhancement of oral bioavailability of poorly water-soluble carvedilol by chitosan nanoparticles: Optimization and pharmacokinetic study. International journal of biological macromolecules. 2019 Aug 15; 135:246-60. https://doi.org/10.1016/j.ijbiomac.2019.05.162
17. Rahim H, Sadiq A, Khan S, Amin F, Ullah R, Shahat AA, Mahmood HM. Fabrication and characterization of glimepiride nanosuspension by ultrasonication-assisted precipitation for improvement of oral bioavailability and in vitro α-glucosidase inhibition. International journal of nanomedicine. 2019 Aug 6:6287-96. https://doi.org/10.2147/IJN.S210548
18. Khan S, Matas MD, Zhang J, Anwar J. Nanocrystal preparation: low-energy precipitation method revisited. Crystal Growth & Design. 2013 Jul 3;13(7):2766-77. https://doi.org/10.1021/cg4000473
19. Verma U, Naik JB, Deshmukh R, Mishra S. Development of biodegradable glimepiride loaded chitosan nano particles: a factorial design approach. Current Environmental Engineering. 2018 Apr 1;5(1):68-77. https://doi.org/10.2174/2212717805666180112161020
20. Mohd AB, Sanka K, Bandi S, Diwan PV, Shastri N. Solid self-nanoemulsifying drug delivery system (S-SNEDDS) for oral delivery of glimepiride: development and antidiabetic activity in albino rabbits. Drug delivery. 2015 May 19;22(4):499-508. https://doi.org/10.3109/10717544.2013.879753
21. Rahim H, Sadiq A, Khan S, Khan MA, Shah SM, Hussain Z, Ullah R, Shahat AA, Ibrahim K. Aceclofenac nanocrystals with enhanced in vitro, in vivo performance: formulation optimization, characterization, analgesic and acute toxicity studies. Drug design, development and therapy. 2017 Aug 23:2443-52. https://doi.org/10.2147/DDDT.S140626
22. Parveen S, Misra R, Sahoo SK. Nanoparticles: a boon to drug delivery, therapeutics, diagnostics and imaging. Nanomedicine in cancer. 2017 Sep 1:47-98.
23. Badar A, Pachera S, Ansari AS, Lohiya NK. Nano based drug delivery systems: present and future prospects. Nanomed Nanotechnol J. 2019;2(1):121.
24. Chandrakala V, Aruna V, Angajala G. Review on metal nanoparticles as nanocarriers: Current challenges and perspectives in drug delivery systems. Emergent Materials. 2022 Dec;5(6):1593-615. DOI: 10.1007/s42247-021-00335-x
25. Mackenzie R, Booth J, Alexander C, Garnett MC, Laughton CA. Multiscale modeling of drug–polymer nanoparticle assembly identifies parameters influencing drug encapsulation efficiency. Journal of Chemical Theory and Computation. 2015 Jun 9;11(6):2705-13. https://doi.org/10.1021/ct501152a
26. Zhang Z, Feng SS. The drug encapsulation efficiency, in vitro drug release, cellular uptake and cytotoxicity of paclitaxel-loaded poly (lactide)–tocopheryl polyethylene glycol succinate nanoparticles. Biomaterials. 2006 Jul 1;27(21):4025-33. https://doi.org/10.1016/j.biomaterials.2006.03.006
27. Cun D, Jensen DK, Maltesen MJ, Bunker M, Whiteside P, Scurr D, Foged C, Nielsen HM. High loading efficiency and sustained release of siRNA encapsulated in PLGA nanoparticles: quality by design optimization and characterization. European journal of pharmaceutics and biopharmaceutics. 2011 Jan 1;77(1):26-35. https://doi.org/10.1016/j.ejpb.2010.11.008
28. Honary S, Ebrahimi P, Hadianamrei R. Optimization of particle size and encapsulation efficiency of vancomycin nanoparticles by response surface methodology. Pharmaceutical development and technology. 2014 Dec 1;19(8):987-98. https://doi.org/10.3109/10837450.2013.846375
29. Zhang X, Xing H, Zhao Y, Ma Z. Pharmaceutical dispersion techniques for dissolution and bioavailability enhancement of poorly water-soluble drugs. Pharmaceutics. 2018 Jun 23;10(3):74. https://doi.org/10.3390/pharmaceutics10030074
30. Kumar R, Dalvi SV, Siril PF. Nanoparticle-based drugs and formulations: current status and emerging applications. ACS Applied Nano Materials. 2020 May 29;3(6):4944-61. https://doi.org/10.1021/acsanm.0c00606
31. Sahu T, Ratre YK, Chauhan S, Bhaskar LV, Nair MP, Verma HK. Nanotechnology based drug delivery system: Current strategies and emerging therapeutic potential for medical science. Journal of Drug Delivery Science and Technology. 2021 Jun 1; 63:102487. https://doi.org/10.1016/j.jddst.2021.102487
32. Narang A, Chang RK, Hussain MA. Pharmaceutical development and regulatory considerations for nanoparticles and nanoparticulate drug delivery systems. Journal of pharmaceutical sciences. 2013 Nov 1;102(11):3867-82. https://doi.org/10.1002/jps.23691
33. Zhou Y, Du J, Wang L, Wang Y. State of the art of nanocrystals technology for delivery of poorly soluble drugs. Journal of Nanoparticle Research. 2016 Sep; 18:1-22. DOI:10.1007/s11051-016-3575-y